significantly more internal motional freedom in Hb than in Mb. Our results show a similar ratio, $\tau_c(Hb)/\tau_c(Mb) = 1.6$, very close to the PAC ratio of 1.4, supporting Marshall's hypothesis. This hypothesis of more motional freedom in HbCO A is significant in that it could originate from a more open heme pocket and result in a less hindered Fe–CO structure and higher CO binding affinity. Indeed, the CO binding affinity of human Hb in the R quaternary state is 4 times greater than that of Mb.[7] (Note that the ^{17}O NMR is probing the R conformation of Hb.) A recent structural analysis[5] also reveals a bent Fe–CO structure, where the bend angles are 165° and 150° for human HbCO and MbCO, respectively, which is consistent with our result of a less hindered HbCO structure.

Our results also provides some evidence on the role of the protein in regulating the CO ligand binding affinities of hemoproteins, especially in solution. We believe an important result emerging from this work is that the size of the heme pocket determines the ligand binding affinities, at least for the CO ligand, of hemoproteins. All of the proteins studied exhibit basically rigid Fe–CO units; however, the motional freedom of the Fe–CO units is different for the different hemoproteins. Thus the hemoproteins with the more open heme pocket provide more room for the CO ligand and/or the heme–CO unit, so they exhibit a less hindered Fe–CO structure (X-ray correlation) and show higher CO binding affinities (Table I).

These results can be summarized as follows: *Picket fence porphyrin*: $\delta_i = 376$, $\nu_{CO} = 1967$ cm^{-1}, linear Fe–C–O, unhindered "pocket", irreversible CO binding. *HbCO A α,β chains (and rabbit HbCO β chains)*: $\delta_i = 369$, $\nu_{CO} = 1951$ cm^{-1}, 165° Fe–C–O bond angle, relatively mobile CO ligand, 0.004 Torr $P_{1/2}$(CO), *Sperm whale MbCO*: $\delta_i = 366.5$, $\nu_{CO} = 1944$ cm^{-1}, 150° Fe–C–O bond angle, hindered/immobile CO "pocket", 0.018 Torr $P_{1/2}$(CO). *Rabbit HbCO α chain*: $\delta_i = 361$, $\nu_{CO} = 1928$ cm^{-1}, rigid CO "pocket", weak CO bonding (in O_2-exchange experiments).

Thus stronger ligand bonding appears to correlate with a more deshielded chemical shift, a higher frequency IR CO stretch frequency, and a more linear Fe–C–O bond angle (where determined), due in large part, we believe, to the packing constraints imposed by the protein (or porphyrin) environment—the larger the constraints, the weaker the bonding, due to deviations from a linear Fe–C–O bond.

Acknowledgment. This work was supported in part by the U.S. National Institutes of Health (Grant HL-19481).

Resonance Raman Spectra of Nitridoiron(V) Porphyrin Intermediates Produced by Laser Photolysis

Wolf-Dieter Wagner and Kazuo Nakamoto*

Contribution from the Department of Chemistry, Todd Wehr Chemistry Building, Marquette University, Milwaukee, Wisconsin 53233. *Received August 22, 1988*

Abstract: Nitridoiron(V) porphyrins, NFeOEP (OEP, octaethylporphinato anion), NFeTPP (TPP, tetraphenylporphinato anion), and NFeTMP (TMP, tetramesitylporphinato anion), were produced by laser irradiation of thin films of the corresponding azido complexes at ~30 K. Formation of the nitrido complexes was detected by the appearance of the ν(Fe≡N) (ν, stretching vibration) at 876 cm^{-1} for the OEP and TPP complexes and at 873 cm^{-1} for the TMP complex in resonance Raman (RR) spectra. These assignments were confirmed by observed frequency shifts due to $^{56}Fe/^{54}Fe$ and $^{14}N/^{15}N$ isotopic substitutions. Frequencies of structure-sensitive bands known for OEP and TPP complexes suggest the Fe(V) state for the nitrido complex and rule out the possibility of π-cation-radical formation. Although the spin state cannot be determined definitively by vibrational spectroscopy, the relatively small Fe≡N stretching force constant (5.07 mdyn/Å) favors the high-spin $(d_{xy})^1(d_{xz})^1(d_{yz})^1$ configuration that was found for isoelectronic oxomanganese(IV) porphyrins. In the case of the OEP complex, RR spectroscopy provides evidence for a reaction scheme in which $NFe^{V}OEP$ is first formed by laser photolysis of the $N_3Fe^{III}OEP$ complex due to low-power irradiation (1–60 mW in the 406.7–514.5-nm range) and subsequently converted to the μ-nitrido dimer $(FeOEP)_2N$ by local heating, which occurred when high laser power (220 mW at 413.1 nm) was applied to the sample. This dimer exhibits the symmetric Fe–N–Fe stretching band at 438 cm^{-1}, which shows expected shifts upon $^{56}Fe/^{54}Fe$ and $^{14}N/^{15}N$ substitutions. Formation of the μ-nitrido dimer is also confirmed by the positions of the structure-sensitive bands in the high-frequency region. The above reaction scheme resembles the autoxidation process of oxyiron porphyrins at low temperature which yields ferrylporphyrins as the intermediate and the μ-oxo dimer as the final product at room temperature.

Extensive research in the past decades has revealed that nature relies on high-valent metalloporphyrins in a number of enzyme-directed processes of biological systems.[1,2] For example, oxygenation reactions catalyzed by cytochrome P-450[3-5] or horseradish peroxidase (HRP)[6,7] involve porphyrin intermediates that contain oxidation states higher than Fe(III). It is generally accepted that the active site of these intermediates is a ferryl moiety (Fe^{IV}=O). Interestingly, the first observation of the ferryl stretching vibration [ν(Fe=O), 852 cm^{-1}] was made for a model compound, O=FeTPP (TPP, tetraphenylporphinato anion)[8,9] by using resonance Raman (RR) spectroscopy. Subsequently, spectroscopic evidence of ferryl formation was obtained via observation of the ν(Fe=O) at 779 cm^{-1} for HRP-II[10,11] and at 797 cm^{-1} for myoglobin.[12] Other high-valent iron porphyrins reported thus far include nitrogen[13] and carbon-bridged[14] dimers which have been proved to

(1) Hewson, W. D.; Hager, L. P. In *The Porphyrins*; Dolphin, D., Ed.; Academic Press: New York, 1979; Vol. 7, pp 295–332.
(2) Griffin, B. W.; Peterson, J. A.; Eastbook, R. W. In *The Porphyrins*; Dolphin, D., Ed.; Academic Press: New York, 1979; Vol. 4, pp 179–256.
(3) Dawson, J. H.; Eble, K. S. *Cytochrome P-450: Heme Iron Coordination Structure and Mechanisms of Action*; Academic Press: New York, 1986; Vol. 4, pp 1–64.
(4) Lewis, D. F. V. *Drug Metab. Rev.* **1986**, *17*, 1–66.
(5) Alexander, L. S.; Goff, H. M. *J. Chem. Educ.* **1982**, *59*, 179–182.
(6) Harami, T.; Maeda, Y.; Morita, Y.; Trautwein, A.; Gonser, U. *J. Chem. Phys.* **1977**, *67*, 1164–1169.
(7) Hanson, L. K.; Chang, C. K.; Davis, M. S.; Fajer, J. *J. Am. Chem. Soc.* **1981**, *103*, 663–670.
(8) Bajdor, K.; Nakamoto, K. *J. Am. Chem. Soc.* **1984**, *106*, 3045–3046.
(9) Proniewicz, L. M.; Bajdor, K.; Nakamoto, K. *J. Phys. Chem.* **1986**, *90*, 1760–1766.
(10) Sitter, A. J.; Reczek, C. M.; Terner, J. *J. Biol. Chem.* **1985**, *260*, 7515–7522.
(11) Hashimoto, S.; Tatsuno, Y.; Kitagawa, T. *Proc. Natl. Acad. Sci. U.S.A.* **1986**, *83*, 2417–2421.
(12) Sitter, A. J.; Reczek, C. M.; Terner, J. *Biochim. Biophys. Acta* **1985**, *828*, 229–235.
(13) Summerville, D. A.; Cohen, I. A. *J. Am. Chem. Soc.* **1976**, *98*, 1747–1752.

0002-7863/89/1511-1590$01.50/0

contain oxidation states 3.5+ and 4+, respectively, by Mössbauer spectroscopy.[15] These compounds were originally regarded as models for probing intradimer exciton coupling and were, therefore, of great interest apart from their unusual electronic and structural properties.[16] Recently, Svastis et al.[17] found that liver microsomal cytochrome P-450-LM3,4 can catalyze the transfer of a functionalized nitrogen atom intramolecularly from a tosylimide analogue of iodosobenzene. In addition the authors reported the successful cytochrome P-450 catalyzed intermolecular transfer and incorporation of a functionalized nitrogen atom into a C–H bond. The proposed reaction cycle involves a high-valent iron porphyrin intermediate with an axial nitrogen ligand.[17] It was, therefore, of great interest to search for model compounds that mimic such an intermediate.

Stable nitridomanganese(V) porphyrins[18,19] and nitridochromium(V) porphyrins,[20] have been prepared by chemical oxidation as well as by photolysis[21,22] and their ν(M≡N) observed at 1049–1052 cm^{-1} for the former[18,20,23] and at 1017 cm^{-1} for the latter.[22] However, no nitridoiron(V) porphyrins had been known prior to our preliminary work,[24] in which we prepared N≡Fe^{V}TPP via laser irradiation (514.5 nm) of N_3Fe^{III}TPP and confirmed its structure by RR spectroscopy. In this paper, we report a more complete result obtained for the analogous OEP (OEP, octaethylporphinato anion) complex. In this case, we were able to establish a reaction scheme in which N≡FeOEP is first formed by laser photolysis of N_3Fe^{III}OEP and subsequently converted to the nitrogen-bridged dimer, $(FeOEP)_2N$, via local heating. We have also included the results on N≡Fe^{V}TPP that were not reported previously and new results on N≡Fe^{V}TMP (TMP, tetramesitylporphinato anion).

Experimental Section

Azidoiron porphyrins (N_3FeOEP, N_3FeTPP, and N_3FeTMP) and their ^{54}Fe, $^{15}N_3$, and $N_2{}^{15}N$ analogues were prepared by the method of Adams et al.[25] H_2OEP, H_2TPP, and H_2TMP were purchased from Midcentury, Posen, IL, and sodium azides containing $^{15}N_3$ and $N_2{}^{15}N$ groups were from ICN Biomedicals, Cambridge, MA. ^{54}Fe was purchased from Oak Ridge National Laboratory, Oak Ridge, TN. Thin films of the azido complexes were prepared by evaporating their methylene chloride solutions on the surface of a copper cold tip which was then cooled down below 30 K by a CTI Model 20/70 cryocooler. RR spectra were recorded on a Spex Model 1403 double monochromator equipped with a Hamamatsu R-928 photomultiplier and a Spex DM1B controller. For RR excitations lines of a Spectra-Physics Model 2025 Ar-ion laser, a Coherent Innova-K3 Kr-ion laser and a Liconix Model 4240 He–Cd laser were used. In order to avoid fast sample decomposition in the laser focus during RR measurements, a backscattering geometry was set up using a small mirror and a cylindrical lens to create a line focus on the sample surface. The line image on the scattering surface was about 4 mm high, thus exposing the thin-film sample to an at least 20-fold lower light density than in the case of a point focus created by a conventional spherical lens. The accuracy of frequency reading was ±1 cm^{-1}.

Electronic absorption measurements were carried out on a Perkin-Elmer Model 320 UV/vis spectrophotometer. Thin films of N_3FeOEP were produced on the window of a Dewar absorption cell by the method described above. The Dewar cell was then cooled to 77 K by liquid nitrogen. The sample area of ≈3 cm^2 was illuminated by the laser, and electronic absorption spectra were recorded between different irradiation periods.

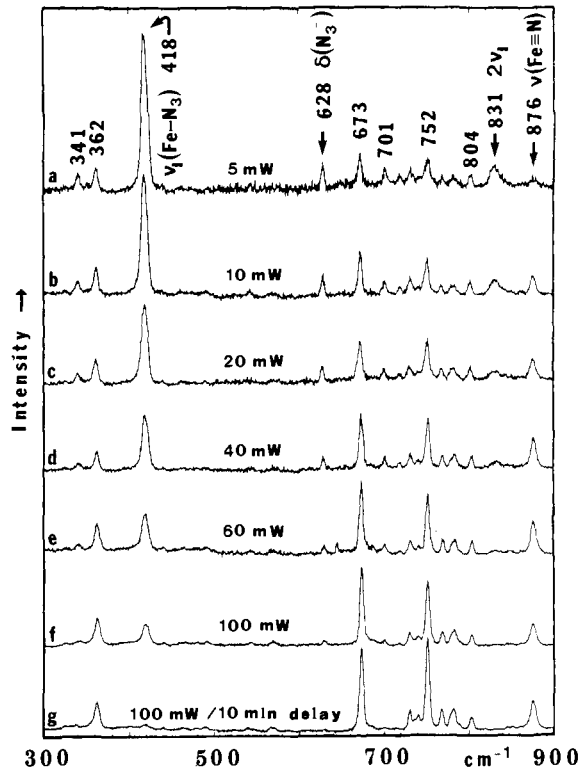

Figure 1. Resonance Raman spectra of a thin film of N_3FeOEP at ≈30 K, 488.0-nm excitation with different excitation power. (a) 5 mW, eight scans added; (b) 10 mW, (four) scans added; (c) 20 mW, two scans added; (d) 40 mW; (e) 60 mW; (f) 100 mW; (g) 100 mW, after 10-min preirradiation with 488.0 nm, 100 mW.

Results and Discussion

OEP Complexes. Photolysis of N_3FeOEP. During RR experiments with a thin film of N_3FeOEP at 30 K, intensity changes of RR bands were observed depending on time and power of irradiation and excitation wavelength. Figure 1 shows a series of RR spectra (488.0-nm excitation) which were obtained from the same N_3FeOEP sample (30 K) with the laser power increasing from 5 (trace a) to 100 mW (trace f). Since intensity changes were noticed during one scan of the 900–300-cm^{-1} region, which took 10 min, the spectra shown in Figure 1 were obtained by connecting three parts (900–700, 700–500, 500–300-cm^{-1} regions) which were recorded separately. Each time a new scan was started a fresh sample spot was in the laser focus. Trace a shows the RR spectrum excited with low laser power (5 mW). Three bands characteristic of the FeN_3 group are readily assignable based on $^{56}Fe/^{54}Fe$ and $^{14}N/^{15}N$ isotopic shifts;[26] ν(Fe–N_3) and its first overtone at 418 and 831 cm^{-1}, respectively, and $\delta(N_3^-)$ (δ, bending vibration) at 628 cm^{-1}. Traces b–f show the RR spectra obtained by using laser power of 10, 20, 40, 60, and 100 mW, respectively. The last spectrum (trace g) is a repetition of the previous scan shown in trace f (100 mW) without changing the irradiated sample spot; thus in this case, a 10-min preirradiation with 100 mW at 488.0 nm was applied. It is seen that the three Fe–N_3 group vibrations mentioned above together with the porphyrin vibrations at 701 and 341 cm^{-1} become weaker, whereas the bands at 876, 752, and 673 cm^{-1} become stronger as the laser power is increased and/or irradiation time is lengthened. As will be shown later (Figure 2), the 876-cm^{-1} band is assigned to the ν(Fe≡N) of N≡Fe^{V}OEP. The remaining bands at 752 and 673 cm^{-1} are attributed to porphyrin modes that are characteristically strong

(14) Mansuy, D.; Lecomte, J.-P.; Chottard, J.-C.; Bartoli, J.-F. *Inorg. Chem.* **1981**, *20*, 3119–3121.
(15) English, D. R.; Hendrickson, D. N.; Suslick, K. S. *Inorg. Chem.* **1983**, *22*, 368–370.
(16) Schick, G. A.; Bocian, D. F. *J. Am. Chem. Soc.* **1983**, *105*, 1830–1838.
(17) Svastis, E. W.; Dawson, J. H.; Breslow, R.; Gellman, S. H. *J. Am. Chem. Soc.* **1985**, *107*, 6427–6428.
(18) Buchler, J. W.; Dreher, C.; Lay, K.-L. *Z. Naturforsch., B: Anorg. Chem., Org. Chem.* **1982**, *37B*, 1155–1162.
(19) Hill, C. L.; Hollander, F. J. *J. Am. Chem. Soc.* **1982**, *104*, 7318–7319.
(20) Buchler, J. W.; Dreher, C.; Lay, K.-L.; Raap, A.; Gersonde, K. *Inorg. Chem.* **1983**, *22*, 879–884.
(21) Tsubaki, M.; Hori, H.; Hotta, T.; Hiwatashi, A.; Ichikawa Y.; Yu, N.-T. *Biochemistry* **1987**, *26*, 4980–4986.
(22) Groves, J. T.; Takahashi, T.; Butler, W. M. *Inorg. Chem.* **1983**, *22*, 884–887.
(23) Campochiaro, C.; Hofmann, J. A., Jr.; Bocian, D. F. *Inorg. Chem.* **1985**, *24*, 449–450.
(24) Wagner, W.-D.; Nakamoto, K. *J. Am. Chem. Soc.* **1988**, *110*, 4044–4045.
(25) Adams, K. M.; Rasmussen, P. G.; Scheidt, W. R.; Hatano, K. *Inorg. Chem.* **1979**, *18*, 1892–1899.
(26) Wagner, W.-D.; Czernuszewicz, R. S.; Nakamoto, K., manuscript in preparation.

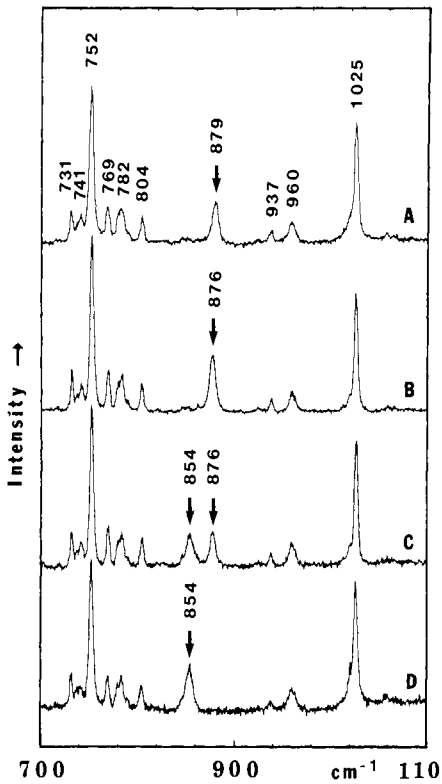

Figure 2. Resonance Raman spectra of the photolysis products of (A) $N_3{}^{54}$FeOEP, (B) N_3FeOEP, (C) $^{15}NN_2$FeOEP + $N_2{}^{15}$NFeOEP in a 1:1 ratio, and (D) $^{15}N_3$FeOEP, thin films at ≈30 K, 488.0 nm, 60 mW.

in the nitrido complex. These results clearly demonstrate that N≡FeOEP is formed as soon as N_3FeOEP at ~30 K is irradiated by the 488.0-nm line (trace a). Upon laser irradiation with 100 mW, the formation of the nitridoiron complex is complete within 10 min (trace g). A spectrum similar to trace g can be obtained even with 5-mW laser power if irradiation is continued over a long time (≈3 h). These observations suggest that the decomposition of N_3FeOEP is caused by photolysis since the concentration of N≡FeOEP thus produced is dependent on the flux of photons reaching the sample surface. This is not surprising as N≡Mn^{V}(PPIX) (PPIX, protoporphyrin IX)[21] and N≡Cr^{V}TTP (TTP, tetra-*p*-tolylporphinato anion)[22] were reportedly formed by photolysis of the corresponding azido complexes. Local heating is unlikely to be responsible for the spectral changes shown in Figure 1 since the same changes were observed when the irradiated thin film was covered with a solid O_2 layer at ≈30 K whose $\nu(O_2)$ was found with constant intensity throughout the RR experiments. If it were due to local heating, the intensity of the $\nu(O_2)$ would have changed due to evaporation of the O_2 layer in the vicinity of the heated porphyrin sample spot. Since the ν(Fe–N_3) at 418 cm^{-1} is one of the dominating bands in the RR spectrum of N_3FeOEP (Figure 1a), it is possible to monitor the progress of photolysis by observing the intensity of this band.

Assignments of ν(Fe≡N) and 2ν(Fe≡N). As stated above, the 876-cm^{-1} band in Figure 1 has been assigned to the ν(Fe≡N) of N≡FeOEP based on isotope shift experiments. Parts A–D of Figure 2 show the RR spectra of photolysis products of N_3FeOEP containing ^{54}Fe, ^{NA}Fe (Fe in natural abundance contains 91.7% ^{56}Fe), $N_2{}^{15}$N, and $^{15}N_3$, respectively. These spectra were obtained by preirradiating the sample spot with 60 mW at 488.0 nm for 20 min. We confirmed before each scan that no bands due to the unreacted azido complex were present. The upward shift in going from 876 (Figure 2B) to 879 cm^{-1} (Figure 2A) indicates that the 876-cm^{-1} vibration involves the motion of the Fe atom. Furthermore, this band is shifted to 854 cm^{-1} by $^{14}N/^{15}N$ substitution (Figure 2D), and the photolysis product of the $N_2{}^{15}N$ azido complex exhibits two bands at 854 and 876 cm^{-1} (Figure 2C). These results provide definitive evidence for our band assignment. The observed shifts (+3 cm^{-1} by $^{56}Fe/^{54}Fe$ substitution and −23 cm^{-1} by $^{14}N/^{15}N$ substitution) are in perfect agreement with theoretical values expected for a Fe≡N diatomic harmonic oscillator.

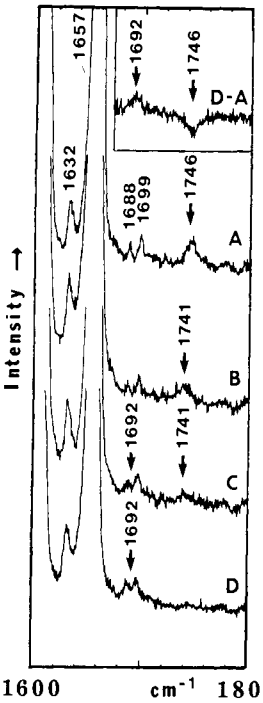

Figure 3. Resonance Raman spectra of the photolysis products of (A) $N_3{}^{54}$FeOEP, (B) N_3FeOEP, (C) $^{15}NN_2$FeOEP + $N_2{}^{15}$FeOEP in a 1:1 ratio, and (D) $^{15}N_3$FeOEP, thin films at ≈30 K, 488.0 nm, 60 mW. Inset shows the difference spectrum of D and A.

The RR spectra of the same isotopomers in the 1800–1600-cm^{-1} region are shown in Figure 3. The weak band at 1741 cm^{-1} (Figure 3B) is assigned to the first overtone of the ν(Fe≡N) at 876 cm^{-1} on the basis of the following observations. This band is shifted to 1746 (Figure 3A) and 1692 cm^{-1} (Figure 3D), respectively, by $^{56}Fe/^{54}Fe$ and $^{14}N/^{15}N$ substitutions, and the photolysis product of the $N_2{}^{15}N$ azido complex shows two bands at 1741 and 1692 cm^{-1} (Figure 3C). The presence of the 1692-cm^{-1} band is not obvious in Figure 3C and D since it is hidden under the porphyrin bands at 1699 and 1688 cm^{-1}. However, the presence of this band can be confirmed by subtracting spectrum A from D as is shown in the inset. The fact that these overtones are observed by 488.0-nm excitation strongly suggests the presence of the Fe–N charge-transfer band near 488.0 nm (vide infra).

Assignments of OEP Vibrations. Thus far, photolysis of N_3FeOEP was carried out by 488.0-nm irradation. It is possible, however, to photolyze N_3FeOEP by other lines in the 406.7–514.5-nm region. For example, the photolysis can be completed in ≈1 min with 413.1-nm irradiation (10 mW) and in ≈20 min with 488.0- or 514.5-nm irradiation (60 mW). RR spectra of NFeOEP can be obtained by using these laser lines after the ν(Fe–N_3) band at 418 cm^{-1} is completely disappeared. The results are shown in Figure 4, The RR spectra recorded with 514.5-(Q) and 413.1-nm (B) excitations are dominated by nontotally and totally symmetric vibrations, respectively. However, complete symmetry classification was not possible since depolarization ratios measured in the film state were of limited value.[27] Thus, band assignments given in Table I were made by comparing our spectra with those of other OEP complexes.[28-31]

(27) Strommen, D. P.; Nakamoto, K. *Appl. Spectrosc.* **1983**, *37*, 436–439.
(28) Hofmann, J. A., Jr.; Bocian, D. F. *J. Phys. Chem.* **1984**, *88*, 1472–1479.
(29) Kitagawa, T.; Ozaki, Y. In *Structure and Bonding 64*; Buchler, J. W., Ed.; Springer Verlag: Berlin, 1987; pp 71–114.
(30) Abe, M.; Kitagawa, T.; Kyogoku, Y. *J. Chem. Phys.* **1978**, *69*, 4526–4534.
(31) Li, X.-L.; Czernuszewicz, R. S.; Kincaid, J. R.; Stein, P.; Spiro, T. G., submitted for publication in *J. Am. Chem. Soc.*

Table I. RR Frequencies (cm^{-1}) and Band Assignments for N_3FeOEP, NFeOEP, and $N(FeOEP)_2$

sym	mode no.[a]	N_3FeOEP[b]	NFeOEP[c]	$N(FeOEP)_2$[d]	$N(FeOEP)_2$[e]	assignment
			In-Plane Skeletal Modes			
A_{1g}	ν_2	1582	1605	1590	1598	$\nu(C_\beta C_\beta)$, $\nu(C_\beta$-Et)
	ν_3	1495	1520	1513	1509	$\nu(C_\alpha C_m)$, $\nu(C_\alpha C_\beta)$
	ν_4	1377	1384	1378	1380	$\nu(C_\alpha N)$, $\delta(C_\alpha C_m)$
		1262	1262	1261		Et(CH_2 twist)
	ν_5	1140	1142	1138		$\nu(C_\alpha C_\beta)$, $\nu(C_\beta$-Et)
		1027	1025	1023	1024	$\nu(C_1$-C_2(Et))
		964	961		959	$\delta(CH_3$(Et))
	$\nu_{33} + \nu_{35}$	732[f]	731	733	731	
	ν_7	672	673	668	671	$\delta(C_\beta C_\alpha N)$, $\nu(C_\alpha C_\beta)$
	ν_8	362	362			$\nu(C_\beta$-Et), $\delta(C_\beta$-Et)
		347		335	341	
B_{1g}	ν_{10}	1631	1657	1647	1646	$\nu(C_\alpha C_m)$, $\nu(C_\alpha C_\beta)$
	ν_{11}		1579			$\nu(C_\beta C_\beta)$, $\nu(C_\beta$-Et)
	ν_{13}	1222	1221	1212	1219	$\delta(C_m H)$, $\nu(C_\alpha C_\beta)$
	ν_{15}	752	752	753	752	$\delta(C_\alpha NC_\alpha)$, $\nu(C_\beta$-Et)
A_{2g}	ν_{19}	1562	1601	1572	1573	$\nu(C_\alpha C_m)$, $\nu(C_\alpha C_\beta)$
	ν_{21}	1310	1311	1312	1313	$\delta(C_m$-H), $\nu(C_\alpha C_\beta)$
	ν_{22}	1130		1132	1136	$\nu(C_\alpha N)$, $\nu(C_\beta$-Et)
B_{2g}	ν_{29}	1409	1412	1405	1409	$\nu(C_\alpha C_\beta)$, $\nu(C_\beta$-Et)
	ν_{30}	1157	1161	1159	1160	$\nu(C_\beta$-Et), $\nu(C_\alpha N)$
			Ligand Vibrations			
		2049[f]				$\nu_{as}(N_3^-)$
		1322[f]				$\nu_s(N_3)$
		628[f]				$\delta(N_3^-)$
		418[f]				ν(Fe-N_3)
			876			ν(Fe≡N)
				439	438	ν_s(Fe-N-Fe)

[a] Mode numbering according to ref 30 and 31. [b] In CH_2Cl_2 at 176 K. [c] Photolysis product of N_3FeOEP thin film at 30 K. [d] In CS_2.[28] [e] Final decomposition product of N_3FeOEP thin film. [f] Thin film at 30 K.

Table I also includes band assignments for N_3FeOEP and $N(FeOEP)_2$. The RR spectrum of N_3FeOEP was obtained by using 488.0-nm excitation with low power (5 mW, see Figure 1a), and the assignments of the Fe–N_3 group vibrations were confirmed by $^{56}Fe/^{54}Fe$ and $^{14}N/^{15}N$ substitutions.[26] Similar spectra were obtained in CH_2Cl_2 solution at 176 K. In this case the ν(Fe–N_3) band at 416 cm^{-1} was the only ligand vibration observed except for a very weak $\nu_{as}(N_3^-)$ band around 2050 cm^{-1}. Since the N_3FeOEP solution was stirred in a Dewar cell (176 K) during the RR experiment, the observed RR frequencies suffered almost no effect of photolysis as fresh sample reached the RR scattering volume continuously. As will be shown later, the final product in the decomposition scheme of N_3FeOEP is the μ-nitrido dimer, $N(FeOEP)_2$. Table I lists the vibrational frequencies of this dimer together with those obtained and assigned by other workers.[28] Vibrational frequencies of most of the bands listed in Table I are very similar among the three compounds. However, large shifts are found for ν_2, ν_3, ν_{10}, and ν_{19}, which are known to be structure-sensitive. Implications of these frequency variations will be discussed in the following section.

Structure-Sensitive Vibrations. Structural information about novel NFeOEP can be obtained by evaluating RR frequencies of several OEP vibrations that are sensitive to the changes in the oxidation and/or spin state.[29,32] Table II lists their frequencies for a series of FeOEP complexes containing different oxidation, spin state, and coordination number. As indicated in Table I, the ν_4 involves in-plane displacements of the pyrrole nitrogen atoms toward the Fe atom. This mode was early recognized as an oxidation-state marker in heme proteins (Band IV),[33] ~1360 cm^{-1} for Fe(II) and ~1375 cm^{-1} for Fe(III). In going from Fe(II) to Fe(III), back-donation of Fe (d) electrons to the porphyrin π^* orbitals decreases, thus strengthening the porphyrin π bonds and raising the ν_4. As seen for a pair of $FeOEP(pip)_2$ and $FeOEP(CO)_2$, strong π-acceptor ligands such as CO also raise the ν_4 since these ligands decrease the π back-donation. Spiro[32] points out that Fe(III) is probably no longer a π donor but rather a π acceptor and proposes that the increase in ν_4 for Fe(IV) (1379 cm^{-1}) reflects the polarization of the pyrrole nitrogen atoms by the nuclear charge falling in the order of Fe(IV) > Fe(III) > Fe(II). Our finding of a still higher ν_4 (1384 cm^{-1}) obtained for NFeOEP fits well into this reasoning and strongly supports the formulation of N≡Fe^{V}OEP together with the observation of the ν(Fe≡N) at 876 cm^{-1}.

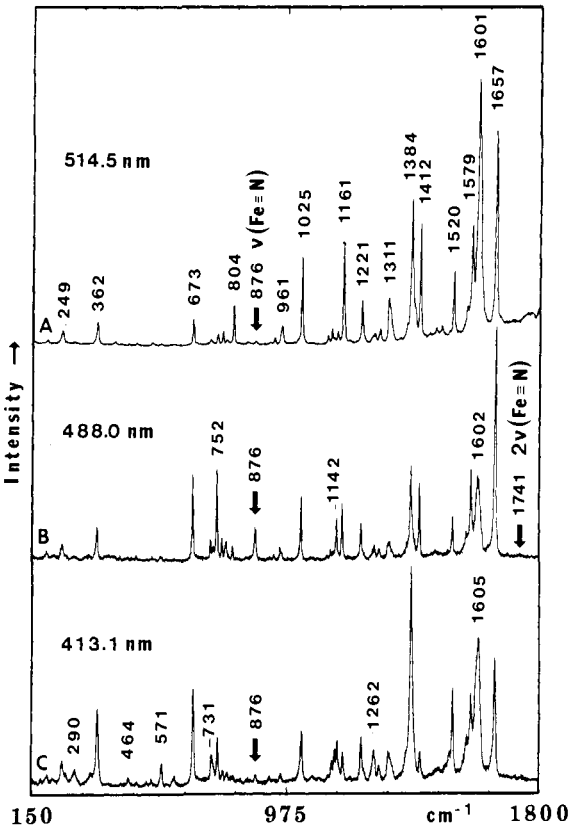

Figure 4. Resonance Raman spectra of the photolysis product of N_3-FeOEP obtained by excitation at (A) 514.5 nm, 80 mW, (B) 488.0 nm 60 mW, and (C) 413.1 nm, 10 mW, thin film at ≈30 K.

(32) Spiro; T. G. In *Iron Porphyrins*; Lever, A. B. P., Gray, H. B., Eds.; Addison-Wesley: Reading, MA, 1983; Part 2, pp 89–159.
(33) Spiro, T. G.; Strekas, T. C. *J. Am. Chem. Soc.* **1974**, *96*, 338–345.

Table II. Oxidation State and Core Size Sensitive RR Bands[a] (cm^{-1}) of FeOEP Derivatives

	spin state	band				
		$\nu_4(A_{1g},p)$	$\nu_3(A_{1g},p)$	$\nu_{19}(A_{2g},ap)$	$\nu_{10}(B_{1g},dp)$	C_t–N, Å
$Fe^{II}OEP(2\text{-}MeIm)$[b]	hs	1359	1488		1608	2.030
$Fe^{II}OEP(pip)_2$[b]	Is	1359	1493		1625	2.020
$Fe^{II}OEP(CO)_2$[b]	Is	1378	1510		1638	1.985
$Fe^{II}OEP$[b]	is	1378	1510		1644	1.980
$Fe^{III}OEPCl$[c]	hs	1376	1494	1565	1628	2.018
$Fe^{III}OEPN_3$[d]	hs	1377	1495	1562	1631	2.017
$Fe^{III}OEP(Im)_2Br$[e]	Is	1378	1506	1589	1640	1.987
$(Fe^{III}OEP)_2O$[c]	hs	1377	1495	1559	1627	2.021
$(Fe^{3.5+}OEP)_2N$[c]	Is	1378	1513	1572	1647	1.986
$(Fe^{3.5+}OEP)_2N$[d]	Is	1380	1509	1572	1646	1.990
$Fe^{IV}OEPO$[b]	Is	1379	1507		1643	1.984
$Fe^{V}OEPN$[d]	hs?	1384	1520	1601	1657	1.956

[a] Mode numbering according to ref 30 and 31. [b] Reference 9. [c] Reference 28. [d] This work. [e] Reference 37. hs, is, and Is denote high spin, intermediate spin, and low spin, respectively.

Other bands listed in Table II are sensitive to the core size of the porphyrin. Originally, Spaulding et al.[34] found a linear relationship between the position of ν_{19} and the center-to-pyrrole-nitrogen distance (C_t–N) of FeOEP complexes. Subsequent investigations[35-37] revealed similar correlations for all skeletal modes above 1450 cm^{-1}. Since the core size of the porphyrin must be adjusted to the spin state of the Fe atom, these bands serve as spin-state marker bands. In high-spin Fe(II) and Fe(III) complexes, the core size increases since electrons occupy the $d_{x^2-y^2}$ orbital. The resulting deformation of the methine bonds (C_α–C_m) causes downshifts of all bands whose normal modes contain substantial $\nu(C_\alpha C_m)$ character. The largest shifts among them are seen in ν^3, ν^{19}, and ν^{10} listed in Table II. From these frequencies, the C_t–N distances can be estimated by using the equation $\nu = k(A - d)$ together with published values of k and A by Ozaki et al.[37] Mean values of the C_t–N distances thus obtained are given in the last column of Table II. The distances calculated from ν_3, ν_{19}, and ν_{10} for the same compound are well within a range of ±0.010 Å except for the dimeric compounds. In the latter case, the C_t–N distances calculated from ν_{19} were 0.02 and 0.04 Å longer than those calculated from ν_3/ν_{10} for the μ-oxo and μ-nitrido complexes, respectively. One possible reason for this discrepancy could be the influence of the ν_{11} band (B_{1g}), which is expected to be close to the assigned ν_{19} band around 1575 cm^{-1}.

The core size of N≡FeOEP was found to be 1.954, 1.962, and 1.952 Å, respectively, based on the observed ν_3, ν_{19}, and ν_{10} frequencies, The average value of 1.956 Å is listed in Table II. This is the smallest C_t–N distance reported thus far for FeOEP complexes. Since these frequencies were obtained at low temperature, comparison of core sizes between $NFe^{V}OEP$ and those OEP complexes listed in Table II must be made with caution. Table II shows that low-spin complexes always have shorter C–N distances than high-spin complexes. In high-valent FeOEP complexes, the C_t–N distance decreases in the order, $N(Fe^{3.5+}OEP)_2$ > $OFe^{IV}OEP$ > $NFe^{V}OEP$. The low-spin state of the μ-nitrido complex was confirmed by X-ray analysis.[38] Thus, the extremely short C_t–N distance observed for NFeOEP is in agreement with a low-spin state. However, the possibility of a high-spin state must be considered as well since a relatively small core size is expected from either the low-spin $(d_{xy})^2(d_{xz})^1$ or the high-spin $(d_{xy})^1(d_{xz})^1(d_{yz})^1$ configuration. The high-spin configuration is comparable to a low-spin $OFe^{IV}OEP$ complex[39] $(d_{xy})^2(d_{xz})^1(d_{yz})^1$ as far as the core size is concerned. As reported earlier,[24] $NFe^{V}OEP$ is isoelectronic with $OMn^{IV}TPP$, and the latter was found to be of high spin by ESR measurements.[40] As pointed out by Czernuszewicz et al.,[40] the half-filled t_{2g} subshell seems to be stabilized via exchange interaction, If so, this might hold for the isoelectronic $NFe^{V}OEP$. However, a π-cation-radical formulation, $NFe^{IV}(OEP^{\bullet})^+$, can be ruled out since large downward shifts of the ν_4 found[41] for OEP and TPP π cation radicals of both types, a_{1u} and a_{2u}, were not observed.

Once the ν(Fe≡N) vibration is identified at 876 cm^{-1} the force constant can be calculated. In the harmonic approximation, this frequency yields a force constant of 5.07 mdyn/Å compared with 4.8 mdyn/Å reported[28] for the FeN bond of $(FeOEP)_2N$. Thus, the FeN bond is only slightly stronger than that of the dimer. This indicates that the FeN bond in NFeOEP is closer to a double bond than to a triple bond which is used in a formal notation. As we pointed out in our preliminary report,[24] occupation of the antibonding d_{xz},d_{yz} orbitals by one (low spin) or two electrons (high spin) causes lowering of the FeN force constant. Comparing both possibilities the FeN bond must be weaker in the high-spin case because the presence of two π^* electrons reduces the bond order from 3 to 2. Thus, the relatively small FeN force constant and the observation of the high-spin state for isoelectronic $OMnTPP$[40] seem to favor the high-spin configuration for NFeOEP. Using Badger's rule,[42] we calculate the equilibrium Fe≡N bond length to be 1.69 Å. The Fe≡N distances were found to be 1.661 and 1.909 Å for $(FeTPP)_2N$[43] and N_3FeTPP[25], respectively, by X-ray analysis. The apparent discrepancy in the FeN distances between the nitrido complex and the dimer is not significant and must be attributed to approximation errors in the equation used and to differences between the porphyrins compared.

Raman Excitation Profile Studies. As seen in Figure 4, the ν(Fe≡N) of NFeOEP is observed by 488.0-nm excitation but hardly seen by excitation at 514.5 and 413.1 nm. To further study the wavelength dependence of RR excitation of the ν(Fe≡N), ν(Fe—N_3), and OEP vibrations, we measured the RR spectra of N_3FeOEP and NFeOEP using 10 exciting lines in the 520–400-nm region. The upper part of Figure 5 shows the Raman excitation profile (REP) of the ν(Fe≡N) obtained from a thin-film sample of N_3FeOEP after the photolysis was completed at 30 K. The $\nu(O_2)$ band from a thin film of O_2 built up on the sample surface was used as the internal (intensity) standard. The data points in the figure were obtained by making reabsorbance correction for backscattering experiments.[44] The lower part presents REPs for ν_5, ν_4, ν_{10}, and ν(Fe–N_3) obtained from a dark solution of N_3FeOEP in CH_2Cl_2. No sign of photodecomposition was noted since the measurements were made by using a stirred Dewar cell

(34) Spaulding, L. D.; Chang, C. C.; Yu, N.-T.; Felton, R. H. *J. Am. Chem. Soc.* **1975**, *97*, 2517–2525.
(35) Spiro, T. G.; Stong, J. D.; Stein, P. *J. Am. Chem. Soc.* **1979**, *101*, 2648–2655.
(36) Choi, S.; Spiro, T. G.; Langry, K. C.; Smith, K. M.; Budd, D. L.; La Mar, G. N. *J. Am. Chem. Soc.* **1982**, *104*, 4345–4351.
(37) Ozaki, Y.; Iriyama, K.; Ogoshi, H.; Ochiai, T.; Kitagawa, T. *J. Phys. Chem.* **1986**, *90*, 6105–6112.
(38) Kadish, K. M.; Bottomley, L. A.; Brace, J. G.; Winograd, N. *J. Am. Chem. Soc.* **1980**, *102*, 4341–4344.
(39) Yamamoto, S.; Teraoka, J.; Kashiwagi, H. *J. Chem. Phys.* **1988**, *88*, 303–312.
(40) Czernuszewicz, R. S.; Su, Y. O.; Stern, M. K.; Macor, K. A.; Kim, D.; Groves, J. T.; Spiro, T. G. *J. Am. Chem. Soc.* **1988**, *110*, 4158–4165.
(41) Czernuszewicz, R. S.; Macor, K. A.; Li, X. Y.; Kincaid, J. R.; Spiro, T. G., submitted for publication in *J. Am. Chem. Soc.*
(42) Herschbach, D. R.; Laurie, V. W. *J. Chem. Phys.* **1961**, *35*, 458–463.
(43) Scheidt, W. R.; Summerville, D. A.; Cohen, I. A. *J. Am. Chem. Soc.* **1976**, *98*, 6623–6628.
(44) Shriver, D. F.; Dunn, J. B. R. *Appl. Spectrosc.* **1974**, *28*, 319–323.

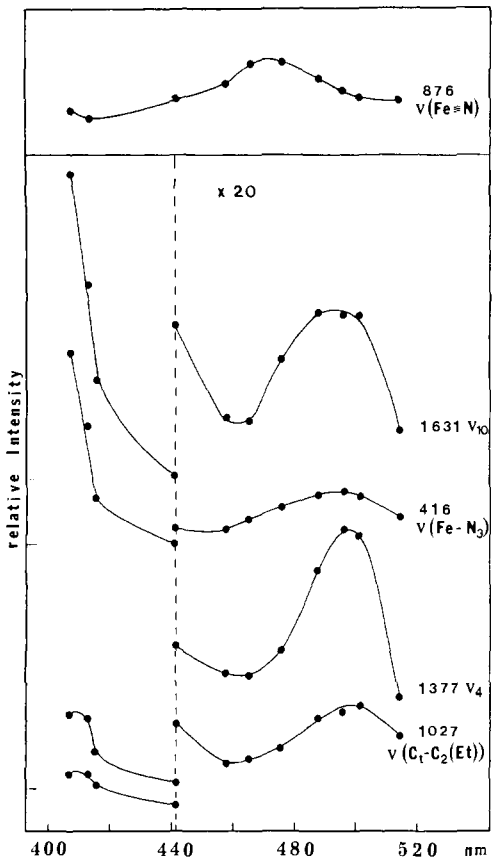

Figure 5. Raman excitation profiles (REPs). Lower part: REPs of N_3FeOEP in methylene chloride solution at 176 K; Raman intensities with Q-band excitation are expanded by a factor of 20 as indicated. Upper part: REP of ν(Fe≡N) of NFeOEP formed by photolysis of N_3FeOEP, thin film ≈30 K.

at 176 K and by applying low laser powers (2–30 mW). In this case, the solvent bands were used as the internal standard.

Figure 6 shows the electronic spectra of N_3FeOEP in CH_2Cl_2 at room temperature (trace a) and of a thin film of N_3FeOEP at 77 K after irradiation with the 488.0-nm line (400 mW) for 0, 30, and 90 min (traces b–d, respectively). In this case a sample area of ≈3 cm^2 was illuminated. Trace d is totally due to NFeOEP as the photolysis is already complete. Traces b and c indicate the spectra of a mixture of N_3FeOEP and NFeOEP in which the latter concentration is increasing in going from b to c. As seen in the lower part of Figure 5, the REP of the ν(Fe–N_3) is similar to those of ν_5, ν_4, and ν_{10}; all these modes exhibit a large maximum in the Soret region and a maximum near 500 nm. These REPs closely follow the electronic spectrum of N_3FeOEP shown in Figure 6a. Thus we conclude that the excitation of the ν(Fe–N_3) vibration occurs via resonance excitation of the porphyrin π–π^* transition which causes a change in the Fe–N_3 distance.[45,32] On the other hand, the REP of the ν(Fe≡N) exhibits a single maximum near 470 nm which is indicated by an arrow in trace d. Since it is far from the porphyrin π–π^* transitions, we conclude that the ν(Fe≡N) is resonance-enhanced via an Fe–N charge-transfer band near 470 nm which is hidden under the strong shoulder of the Soret band at 395 cm^{-1}.

Decomposition Scheme of N_3FeOEP. As stated earlier, irradiation of N_3FeOEP at 488.0 nm with low laser power produces NFeOEP. However, continued irradiation of the same sample with excitation wavelengths near the Soret band and with laser powers higher than 120 mW produces the third species, which can be assigned to the μ-nitrido dimer $(FeOEP)_2N$. Figure 7 represents a complete series of spectral changes observed in the 900–300-cm^{-1} region. Trace A shows the RR spectrum of a thin film of N_3FeOEP at ~30 K irradiated with 5 mW of 488.0-nm line. This spectrum is identical with that shown in Figure 1a; it is the RR spectrum of almost pure N_3FeOEP. As seen in Figure 7B, this sample is converted to NFeOEP after 20-min irradiation of the 488.0-nm line with 60 mW. Parts C and D, of Figure 7 show the RR spectra from the same sample spot obtained by switching the excitation line to 476.2 nm (60 mW) and to 413.1 nm (10 mW), respectively. The ν(Fe≡N) of NFeOEP at 876 cm^{-1} is the strongest with 476.2-nm excitation, indicating that the Fe–N charge-transfer transition mentioned above lies near 476 nm. The spectrum shown in Figure 7E was obtained by increasing the laser power of the 413.1-nm line from 10 mW (Figure 7D) to 220 mW. It is seen that the 876-cm^{-1} band disappears completely and a new set of bands emerges at 798, 438, and 341 cm^{-1}.

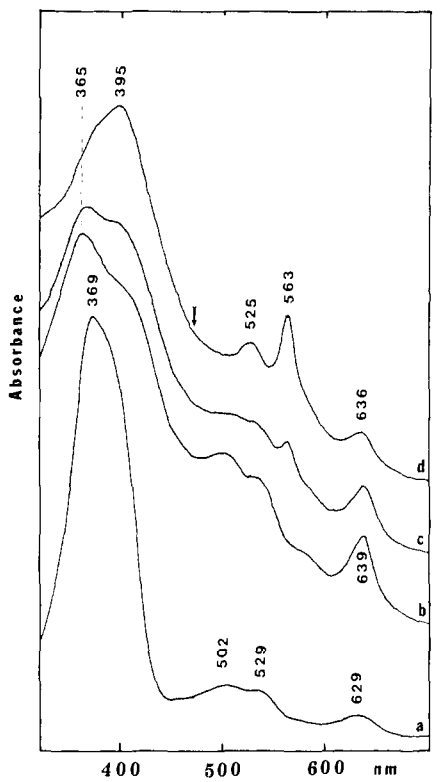

Figure 6. Electronic absorption spectra of (a) N_3FeOEP in methylene chloride, (b) N_3FeOEP, thin film at 77 K, (c) as (b) after 30 min of 488.0-nm, 400-mW irradiation, (d) as (b) after 90 min of 488.0-nm, 400-mW irradiation, illuminated sample area ≈3 cm^2.

The new band at 438 cm^{-1} is of particular interest. Figure 8 compares the RR spectra of $N_3{}^{54}FeOEP$, N_3FeOEP, and $^{15}N_3$-FeOEP which were excited at 413.1 nm with 220-mW laser power. It is seen that this band shifts up 6 cm^{-1} upon $^{56}Fe/^{54}Fe$ substitution but shows little shift upon $^{14}N/^{15}N$ substitution. These results clearly indicate that the 438-cm^{-1} band is due to the symmetric stretching vibration of a linear Fe–N–Fe bridge.[43] Previously, Hofmann and Bocian[28] prepared $(FeOEP)_2N$ by chemical methods and assigned the 439-cm^{-1} band (CS_2 solution) to the ν_s(Fe–N–Fe) on the basis of the observed upshift of 6 cm^{-1} upon $^{56}Fe/^{54}Fe$ substitution (from 439 to 445 cm^{-1}). Thus, our ν_s(Fe–N–Fe) value obtained in the film state is in perfect agreement with that value reported by these authors.

Figure 9 shows the spectral changes in the high-frequency region as part of the same series of experiments shown in Figure 7. Trace A is the RR spectrum of N_3FeOEP irradiated by the 488.0-nm line with 5 mW. Photolysis effects are already noticeable, as two ν_{10} bands appear at 1632 (azido complex) and 1657 cm^{-1} (nitrido complex). The $\nu_s(N_3^-)$ of the azido group is still seen at 1322 cm^{-1}. With more intense 488.0-nm excitation (60 mW), this band and the band at 1632 cm^{-1} disappear completely after 20 min (Figure 9B). The intensities of the nitrido bands at 1657 (ν_{10}) and 1412 cm^{-1} (ν_{29}) decrease upon switching the exciting line from 488.0 to 413.1 nm and applying low power (10 mW) to the thin-film

(45) Kitagawa, T.; Abe, M.; Kyogoku, Y.; Ogoshi, H.; Watanabe, E.; Yoshida, Z. *J. Phys. Chem.* **1976**, *80*, 1181–1186.

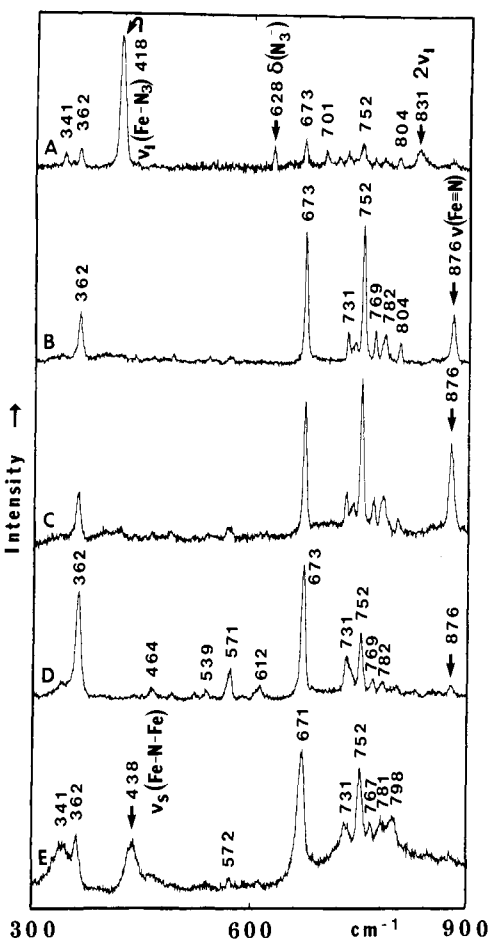

Figure 7. Resonance Raman spectra of N_3FeOEP, thin film at ≈30 K, obtained from the same sample spot demonstrating spectral changes caused by laser irradiation, low-frequency region. (A) 488.0-nm excitation, 5 mW, 10 scans added; (B) 488.0-nm excitation, 60 mW, after 20 min of 488.0-nm, 60-mW irradiation; (C) 476.2-nm excitation, 60 mW; (D) 413.1-nm excitation, 10 mW; (E) 413.1-nm excitation, 220 mW.

sample (Figure 9C). When the laser power is increased to 220 mW, structure-sensitive bands such as ν_4 (1384 cm^{-1}), ν_3 (1520 cm^{-1}), and ν_{10} (1657 cm^{-1}) are shifted to lower frequencies, as seen in Figure 9D. Table I compares these frequencies with those obtained in CS_2 solution by Hofmann and Bocian.[28] It should be kept in mind that the compared frequencies were obtained under different conditions and that the formation of $(FeOEP)_2N$ is not complete in our case. This is indicated, for example, by the presence of the 362-cm^{-1} band of N≡FeOEP, which is still visible in Figure 7E, and by several shoulder bands due to N≡FeOEP, which remain on the high-frequency sides of the structure-sensitive bands of the μ-nitrido dimer shown in Figure 9D. Nevertheless, the agreement between both results is good except for ν_2, which is found to be 8 cm^{-1} higher in our case. This could be due to an overlap with the remainder of the 1605-cm^{-1} band of NFeOEP.

The results described above suggest the following decomposition scheme:

$$N_3\text{—}Fe^{III}(OEP) \xrightarrow{h\nu} N{\equiv}Fe^{V}(OEP) \xrightarrow{\Delta} (OEP)Fe^{3.5+}\text{—}N\text{—}Fe^{3.5+}(OEP)$$

We have already shown that step 1 is the photolysis of N_3-FeOEP to N≡FeOEP by laser irradiation in the 413.1–514.5-nm region and that 488.0-nm excitation is well suited for detecting the formation of N≡FeOEP. Under our experimental conditions, step 2 can occur when irradiation is made at 413.1 nm with power exceeding 120 mW. We found, however, that the critical laser power depends on the thickness of the irradiated thin film. These observations strongly suggest that step 2 depends on the temperature. In this case, it is the equilibrium temperature built up at the sample surface during laser irradiation. This temperature

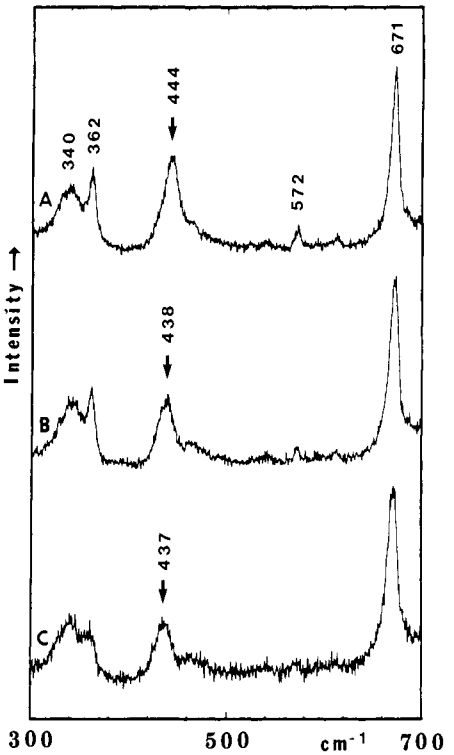

Figure 8. Resonance Raman spectra of the laser induced decomposition products of (A) $N_3{}^{54}$FeOEP, (B) N_3FeOEP, (C) $^{15}N_3$FeOEP, thin films at ≈30 K, 413.1 nm excitation, 220 mW.

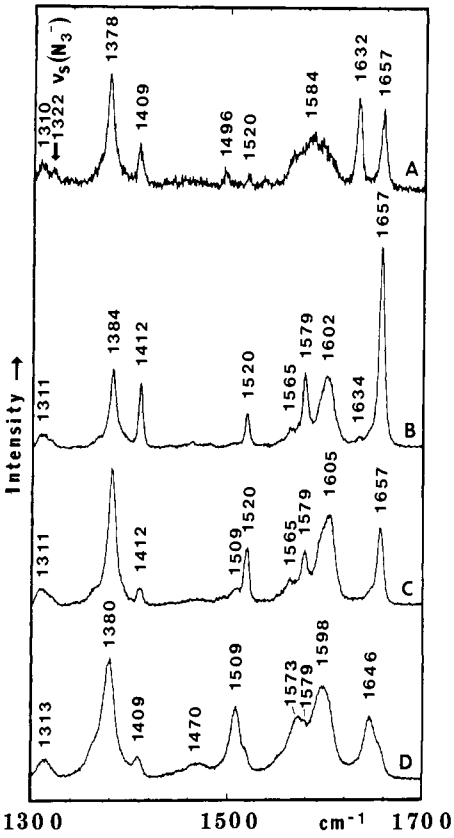

Figure 9. Resonance Raman spectra of N_3FeOEP, thin film at ≈30 K, obtained from the same sample spot demonstrating spectral changes caused by laser irradiation, high-frequency region. (A) 488.0-nm excitation, 5 mW, 10 scans added; (B) 488.0-nm excitation, 60 mW, after 20 min of 488.0-nm, 60-mW irradiation; (C) 413.1-nm exciation, 10 mW; (E) 413.1-nm excitation, 220 mW.

Table III. Oxdiation State and Core Size Sensitive RR Bands[a] (cm^{-1}) of FeTPP Derivatives

		band					
	spin state	$\nu_4(A_{1g},p)$,A	$\nu_{29}(B_{2g},dp)$,B	$\nu_3(A_{1g},p)$	$\nu_{20}(A_{2g},ap)$,C	$\nu_2(A_{1g},p)$,D	C_t-N, Å
$Fe^{II}TPP$[b]	is	1367			1540	1565	1.991
$Fe^{II}TPP(pip)_2$[b]	Is	1355			1540	1560	1.996
$Fe^{III}TPPCl$[c]	hs	1367	1373	1454	1518	1559	2.014
$Fe^{III}TPPN_3$[c]	hs	1364	1373	1452	1520	1555	2.020
$Fe^{III}TPP(Im)_2Cl$[d]	Is	1370		1456	1540	1568	1.988
$(Fe^{III}TPP)_2O$[e]	hs	1359	1368	1450	1511	1553	2.027
$(Fe^{3.5+}TPP)_2N$[f]	Is	1367	1374		1538	1567	1.990
$(Fe^{IV}TPP)_2C$[g]	Is	1370	1377		1539	1571	1.981
$Fe^{IV}TPPO$[h]	Is	1374				1575	1.950
$Fe^{V}TPPN$[c]	hs?	1373	1378	1472	1552	1576	1.956

[a] Mode numbering according to ref 50, 30, and 31. [b] Reference 48. [c] This work. [d] Reference 49. [e] Reference 50. [f] Reference 16. hs, is, and Is denote high spin, intermediate spin, and low spin, respectively.

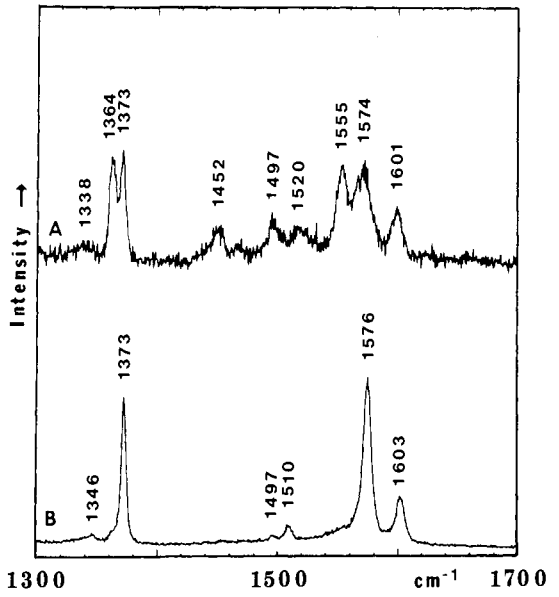

Figure 10. Resonance Raman spectra of N_3FeTPP excited with (A) 488.0-nm, 2-mW, 10 scans added, and (B) 488.0-nm, 60 mW, thin film at ≈30 K.

is a function of the thickness of the absorbing layer since the latter acts as thermal insulator against the cooling head. Thus, we conclude that step 2 proceeds via local heating, which increases the contact of the nitrido complex with its decomposition product FeOEP. Previously, Summerville and Cohen[13] prepared $(FeTPP)_2N$ by refluxing N_3FeTPP in xylene under nitrogen atmosphere for 14 h. Subsequently $(FeOEP)_2N$ was prepared by the same method.[28] In this work, we were able to produce and stabilize $NFe^{V}OEP$ as an intermediate in a decomposition reaction of N_3FeOEP (thin film) induced by laser irradiation. This intermediate is likely to be involved in the above procedure,[28] where the μ-nitrido dimer is formed in solution, as well. Interestingly, the reaction scheme established here for the decomposition of N_3FeOEP is similar to the oxidation reaction of ferrous porphyrins where ferrylporphyrin is the precursor to the formation of the μ-oxo dimer.[46]

TPP Complexes. In the previous paper,[24] we reported that N≡FeTPP formed by laser photolysis of N_3FeTPP exhibits the ν(Fe≡N) at 876 cm^{-1}. As shown in the preceding section, it takes ~20 min to complete the photolysis of N_3FeOEP with 488.0-nm excitation (60 mW). However, the photolysis of N_3FeTPP proceeds much faster. Figure 10 compares the RR spectra of N_3-FeTPP obtained by low (2 mW, trace A) and high laser power (60 mW, trace B), both with 488.0-nm excitation. The bands at 1555 (ν_2) and 1364 (ν_4) of N_3FeTPP are completely absent and only those of N≡FeTPP at 1576 (ν_2) and 1373 cm^{-1} (ν_4) remain in trace B. This result indicates that the photolysis of N_3FeTPP is complete as soon as a thin film of N_3FeTPP is irradiated by the 488.0-nm line with 60 mW.

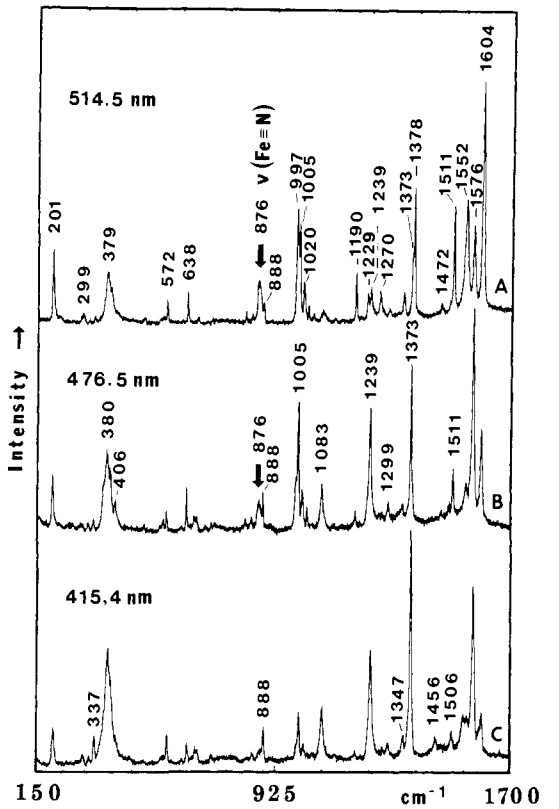

Figure 11. Resonance Raman spectra of the photolysis product of N_3-FeTPP excited with (A) 514.5 nm, 80 mW, (B) 476.5 nm, 60 mW, and (C) 415.4 nm, 2 mW, thin film at ≈30 K.

Figure 11 shows the RR spectra of N≡FeTPP obtained by three different exciting lines. These spectra were taken after the photolysis was completed. The resonance enhancement maximum of the ν(Fe≡N) at 876 cm^{-1} seems to be shifted to longer wavelengths in comparison with NFeOEP, as can be seen from the RR spectra obtained with 514.5-, 476.5-, and 415.4-nm excitation (Figure 11). It was not possible, however, to study the REP of the ν(Fe≡N) since the porphyrin band at 869 cm^{-1} is hidden under the 876-cm^{-1} band. Therefore, the trend mentioned above could not be confirmed.

Previously, Spiro et al.[47] and Chottard et al.[48] had shown that FeTPP complexes exhibit at least five RR bands which reflect the oxidation state and coordination number of the iron center and the core size of the porphyrin. These bands ν_4 (1373 cm^{-1}), ν_{29} (1378 cm^{-1}), ν_3 (1472 cm^{-1}), ν_{20} (1552 cm^{-1}), and ν_2 (1576

(46) Chin, D.-H.; Del Gaudio, J.; La Mar, G. N.; Balch, A. L. *J. Am. Chem. Soc.* **1977**, *99*, 5486–5488.

(47) Stong, J. D.; Spiro, T. G.; Kubaska, R. J.; Shupack, S. I. *J. Raman Spectrosc.* **1980**, *9*, 312–314.

(48) Chottard, G.; Battioni, P.; Battioni, J.-P.; Lange, M.; Mansuy, D. *Inorg. Chem.* **1981**, *20*, 1718–1722.

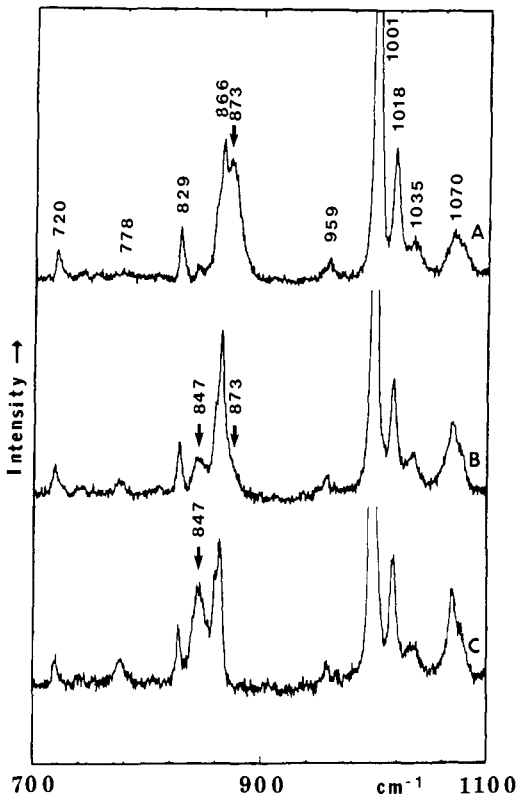

Figure 12. Resonance Raman spectra of the photolysis products of (A) N_3FeTMP, (B) $^{15}NN_2FeTMP + N_2{}^{15}NFeTMP$ in a 1:1 ratio, and (C) $^{15}N_3FeTMP$, thin films at ≈30 K, 514.5-nm, 80-mW excitation.

cm^{-1}) can be identified in Figure 11 by comparing with RR spectra of other FeTPP complexes[47-50] and by observing differences in polarization properties. Table III lists the frequencies of these five bands for a series of FeTPP complexes having different oxidation state, spin state, and coordination number. The mode numbers used are those of Stein and Spiro,[50] who followed those given by Abe et al.[30] in their assignments of NiOEP. The designations given by Chottard et al.[48] are also shown in Table III. As in the case of OEP complexes, ν_4 reflects the oxidation state, which is governed by the degree of π back-donation. This band is also sensitive to the change in the spin state[45] as seen in the comparison of Fe(II) complexes having high- and low-spin states. As to five-coordinate low-spin complexes, an increase in ν_4 is noted in going from Fe(3.5+) to Fe(IV). However, the ν_4 of the Fe(IV) and Fe(V) complexes are almost the same. This is different from the case of OEP complexes where the ν_4 of $NFe^{V}OEP$ is 5 cm^{-1} higher than that of $OFe^{IV}OEP$. As seen in Tables II and III, the variation of ν_4 is 26 cm^{-1} in the case of OEP, whereas it is only 18 cm^{-1} in the case of TPP when the respective $(pip)_2$ and nitrido complexes are compared. Thus, the ν_4 of NFeTPP should be closer to that of OFeTPP when compared with the respective OEP complexes. Limited experimental accuracy also adds to the observed small difference between the ν_4 of the OEP and TPP nitrido complexes.

The ν_{29} (or B) is a marker band for pentacoordination, which is observable only by Q-band excitation.[48] Observation of this band at 1378 cm^{-1} for N≡FeTPP thus confirms pentacoordination of the sample studied here. The remaining three bands listed in Table III serve as core-size markers as in the case of OEP complexes. Stong et al.[47] found linear relationships between these frequencies and the C–N distance and derived a similar empirical equation as given in the preceding section. The C_t–N distances shown in the last column of Table III were calculated by using their equation with given K and A values. The results are similar to that of the OEP complexes (Table II). The core sizes of low-spin complexes are small and decrease with increasing oxidation state of the Fe atom. The core size of NFeTPP is the same as that of NFeOEP (1.956 Å). However, the core size of OFeTPP (1.950 Å) is found to be smaller than that of OFeOEP (1.984 Å). This suggests that the frequency reported for ν_4 of OFeTPP is perhaps on the upper limit of the instrumental error. Thus, we propose a $NFe^{V}TPP$ formulation and the same argumentation presented for $NFe^{V}OEP$ concerning its spin state.

As stated earlier, irradiation of N_3FeOEP by the 413.1-nm line with high power (220 mW) produced the μ-nitrido dimer as a result of local heating in the film state. Formation of such a dimer has not been confirmed yet for the TPP complex. This is in part due to the fact that RR enhancement of axial ligand vibrations of N_3FeTPP and $N(FeTPP)_2$ is weaker than those of the respective OEP complexes, thus rendering vibrational identifications more difficult. Alternatively, evaporation of the irradiated samples starts at much lower laser power for TPP complexes than for OEP complexes in the wavelength range 406.7–514.5 nm studied here. Thus, the local temperature needed to form the dimer might not be reached in case of the TPP complexes.

TMP Complexes. Parts A–C of Figure 12 show the spectra of photolysis products of N_3FeTMP (TMP, tetramesitylporphinato anion) containing the N_3, $N_2{}^{15}N$, and $^{15}N_3$ ligands, respectively. The band at 873 cm^{-1} is shifted to 847 cm^{-1} by $^{14}N/^{15}N$ substitution, and the $N_2{}^{15}N$ compound exhibits both of these bands. These results clearly indicate that the 873-cm^{-1} band is the ν(Fe≡N) of N≡FeTMP. In the high-frequency region, the bands analogous to the ν_4 and ν_2 of NFeTPP appear at almost the same frequencies. However, no indication of the μ-nitrido dimer formation was noted even by irradiation of the 413.1-nm line with high laser power. This is in agreement with the notion that steric hindrance caused by the o-methyl groups of TMP prevents such a dimerization.

Acknowledgment. This work was supported by the National Science Foundation (DMB-8613741). W.-D.W. is a recipient of a Feodor Lynen Fellowship from the Alexander von Humboldt Foundation. We thank Drs. R. S. Czernuszewicz, T. G. Spiro, and J. R. Kincaid for showing their manuscripts prior to publication.

(49) Burke, J. M.; Kincaid, J. R.; Peters, S.; Gagne, R. R.; Collman, J. P.; Spiro, T. G. *J. Am. Chem. Soc.* **1978**, *100*, 6083–6088.
(50) Stein, P.; Ulman, A.; Spiro, T. G. *J. Phys. Chem.* **1984**, *88*, 369–374.
(51) Hofmann, J. A., Jr.; Bocian, D. F. *Inorg. Chem.* **1984**, *23*, 1177–1180.